Journal Name

ARTICLE TYPE

Cite this: DOI: 00.0000/xxxxxxxxxx

Tailored self-assembled nanocolloidal Huygens scatterers in the visible

Rajam Elancheliyan,[a] Romain Dezert,[a] Sabine Castano,[b] Ahmed Bentaleb,[a] Einat Nativ-Roth,[c] Oren Regev,[c,d] Philippe Barois,[a] Alexandre Baron,*[a] Olivier Mondain-Monval[a] and Virginie Ponsinet*[a]

Received Date
Accepted Date

DOI: 00.0000/xxxxxxxxxx

1 Supplementary Information

1.1 Size distribution of the gold nanoparticles

The size distribution of the particles was determined by SAXS to correspond to a Gaussian distribution with mean radius $r = 6.7$ nm and standard deviation $\sigma = 1$ nm. We also imaged the nanoparticles by standard TEM (see Figure S1 and found a compatible size distribution by image analysis, as shown on Figure Fig.S2.

1.2 Ripening of the emulsions

During the PVP-NPs emulsion ripening process, we sampled aliquots at different intervals of time (15 min, 30 min, 45 min, and 75 min) and also sampled the suspension after 75 min of ripening and two days of stirring in a dry atmosphere at normal pressure, to study the structure of the droplets. These samples were labelled PVP-R15, PVP-R30, PVP-R45, PVP-R75 and PVP-R75V2, respectively, and were studied using both UV-Visible and IR spectroscopies.

ATR-FTIR spectra were taken for samples PVP-R15, PVP-R30, PVP-R45, PVP-R75 and are shown on Fig.S3. For the aliquots sampled first, intense bands at 1650 and 3480 cm^{-1} were identified as related to the water molecules. As ripening occurs, we observe a clear decrease of these two bands, indicating that water evaporates from the sample. An ATR-FTIR spectrum was also taken for sample PVP-R75V2 but did not display the water bands, showing that water had been fully removed after this level of ripening, at least up to the detection limit of the spectrometer (data not shown).

1.3 Simulations of scattering efficiency

We calculated the multipolar decomposition of the scattering efficiency for a sphere of radius 100 nm composed of a Maxwell Garnett medium of gold volume fraction f (see Figure S4). We see that the magnetic quadrupolar term is always negligible, and that the electric dipolar term becomes double-peaked at high volume fraction.

1.4 Polarization resolved light scattering

The measured perpendicular and parallel signals $I_{SV}(\phi)$ and $I_{SH}(\phi)$ for sample PEG800/40-NPs are plotted on the Figure S5 at a wavelength of 660 nm, and fitted to simple functions:

$$\begin{cases} I_{SV}(\phi) = A_V \sin^2\phi + B \\ I_{SH}(\phi) = A_H \cos^2\phi + B \end{cases} \quad (1)$$

The background signal B, identical for both functions, does not exceed a few percent (at most 5% across the wavelength range) of the amplitude A_V, which fully validates the assumption of isotropic scatterers[1]. The values of A_H and A_V are extracted for all studied wavelengths, and their ratio is plotted as a function of wavelength on Figure 6.b in the

[a] Univ. Bordeaux, CNRS, Centre de Recherche Paul Pascal, UMR 5031, F-33600 Pessac, France, E-mail: alexandre.baron@u-bordeaux.fr, virginie.ponsinet@crpp.cnrs.fr
[b] Institut de Chimie et Biologie des Membranes et des Nano-objets, Univ. Bordeaux, CNRS, INP, UMR 5248, F-33600 Pessac, France.
[c] Department of Chemical Engineering, Ben Gurion University of the Negev IL-84105 Beer Sheva, Israel.
[d] Ilse Katz Institute for Nanoscale Science and Technology, Ben Gurion University of the Negev IL-84105 Beer Sheva, Israel.

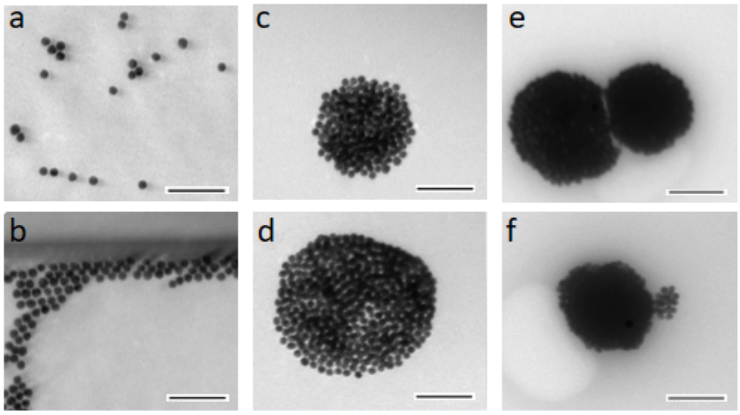

Fig. S1 Standard TEM images of (a,b) initial gold nanoparticles, (c,d) PVP-clusters and (e,f) PEG2000/40 clusters. Flattening (d) or aggregation (e) of the clusters are likely artifacts due to the drying of the suspensions on the supporting grids. Bars = 100 nm.

main text.

Notes and references

1 S. Gomez-Graña, M. Treguer-Delapierre, E. Duguet, J.-B. Salmon, J. Leng, V. Kravets, A. N. Grigorenko, A. Peyyety, V. Ponsinet, P. Richetti *et al.*, 2016 10th International Congress on Advanced Electromagnetic Materials in Microwaves and Optics (METAMATERIALS), IEEE, 2016, pp. 52–54.

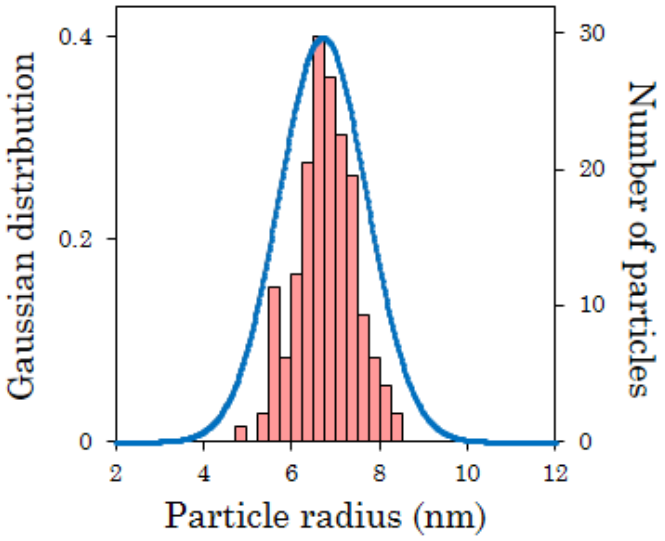

Fig. S2 Size distribution of the gold NPs. Gaussian distribution of radius $r = 6.7$ nm and standard deviation $\sigma = 1$ nm as extracted by the Small-Angle X-ray Scattering study of a NP suspension (blue line, left axis) and histogram of size determined on TEM images for 200 NPs (pink rectangles, right axis).

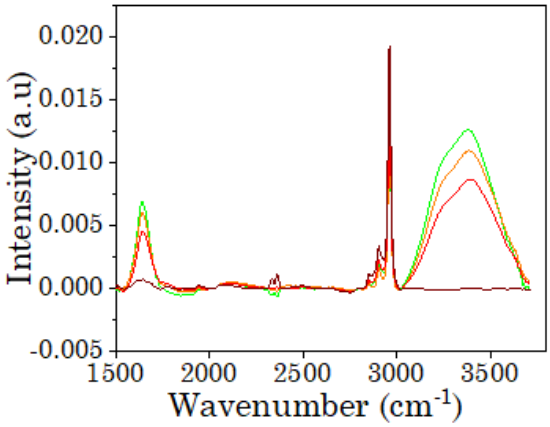

Fig. S3 ATR-FTIR spectra of samples PVP-R15 (green), PVP-R30 (orange), PVP-R45 (red), and PVP-R75 (brown)

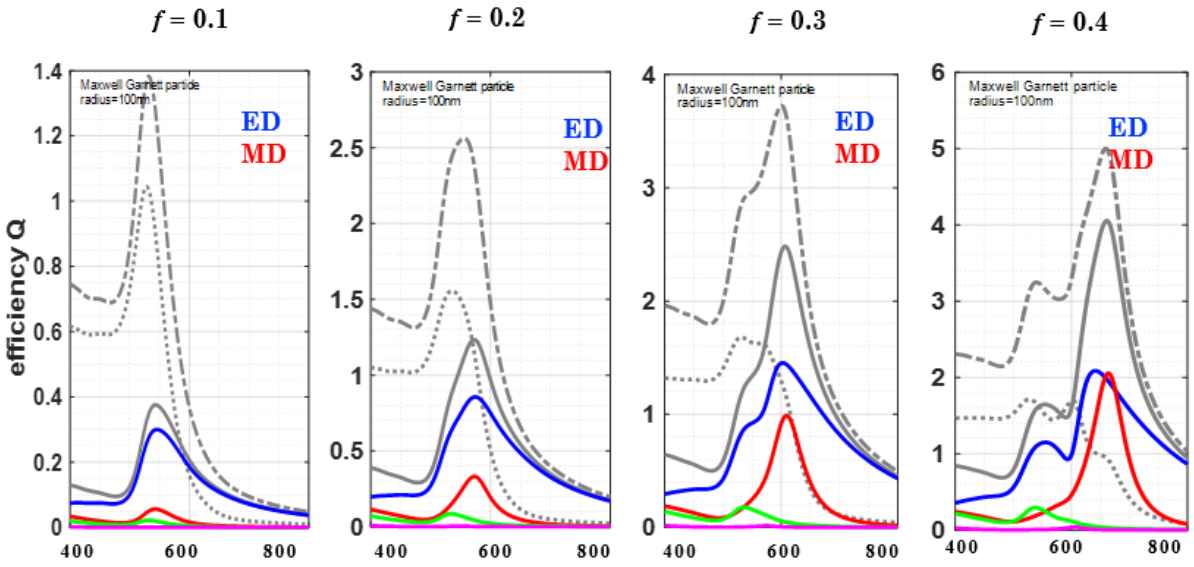

Fig. S4 Simulations of the scattering and absorption efficiencies for different gold volume fraction f in a cluster of radius 100 nm, considered as a Maxwell Garnett medium. The total scattering efficiency (full gray line) can be decomposed into the electric dipolar component (blue), magnetic dipolar component (red), electric quadrupolar component (green), magnetic quadrupolar component (pink, very close to zero). The absorption efficiency is also plotted (dotted gray line), as well as the extinction efficiency (sum of scattering and absorption, dashed-dotted gray line).

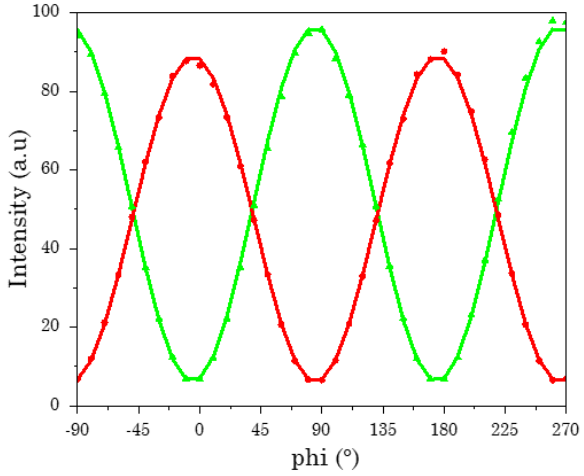

Fig. S5 Measured intensity (symbols) as a function of the incident polarization angle ϕ for sample PEG800/40-NPs with output polarizations perpendicular (green triangles) and parallel (red circles) to the scattering plane at a wavelength $\lambda = 660$ nm and a scattering angle $\theta = 90°$. Simple fits (lines) of $A_V \sin^2\phi + B$ (green) and $A_H \cos^2\phi + B$ (red).